August 2013

Efficacy of Gold Silica Nanoshells and Gold Nanorods for Photothermal Therapy of Human Glioma Spheroids

Suyog Jung Chhetri
University of Nevada, Las Vegas

EFFICACY OF GOLD SILICA NANOSHELLS AND GOLD NANORODS FOR PHOTOTHERMAL THERAPY OF HUMAN GLIOMA SPHEROIDS

By

Suyog Chhetri

Bachelor of Science in Radiological Health Science
Purdue University, West Lafayette
2009

A thesis submitted in partial fulfillment
of the requirements for the

Master of Science in Health Physics

Department of Health Physics
School of Allied health Sciences
The Graduate College

University of Nevada, Las Vegas
August 2013

UNLV
UNIVERSITY OF NEVADA LAS VEGAS

THE GRADUATE COLLEGE

We recommend the thesis prepared under our supervision by

Suyog Chhetri

entitled

Efficacy of Gold Silica Nanoshells and Gold Nanorods for Photothermal Therapy of Human Glioma Spheroids

be accepted in partial fulfillment of the requirements for the degree of

Master of Science – Health Physics
Department of Health Physics

Steen J. Madsen, Ph.D., Committee Chair

Ralf Sudowe, Ph.D., Committee Member

Gary Cerefice, Ph.D., Committee Member

Patricia T. Alpert, Ph.D., Graduate College Representative

Kathryn Hausbeck Korgan, Ph.D., Interim Dean of the Graduate College

August 2013

ABSTRACT

Efficacy of Gold Silica nanoshells and Gold NanoABSTrods for Photothermal Therapy of Human Glioma Spheroids

By

Suyog J. Chhetri

Dr. Steen Madsen, Examination Committee Chair
Chair, Professor of Health Physics and Diagnostic Sciences
University of Nevada, Las Vegas

Gold-based nanoparticles including gold-silica nano-spheres and gold nano-rods have been investigated for a number of therapeutic and diagnostic applications. The ability of these nanoparticles to convert light into heat energy makes them particularly appealing for photothermal therapy in which cancer cells are destroyed via light-induced heat generation. The overall objective of the study is to compare the efficacy of gold-silica nano-spheres and gold nano-rods in an *in vitro* system consisting of human brain tumor (glioma) spheroids.

Delivery of the nanoparticles to the spheroids was accomplished using murine macrophages. Nanoparticles (spheres or rods) were incubated with macrophages for 24 hours. Thereafter, nanoparticle-loaded macrophages were combined with human glioma cells and centrifuged in order to create a hybrid spheroid. Approximately 48 hours post centrifugation, the resultant 400 μm dia. spheroids were exposed to 808 nm laser light for 10 min at irradiances of 2, 7, 14 and 28 W cm^{-2}. Treatment efficacy was evaluated from spheroid growth kinetics over a 14-day period.

Gold nanoshells were shown to have greater efficacy compared to gold nanorods. For example, hybrid spheroids consisting of a 5:1 ratio of glioma cells to nanosphere-

loaded macrophages exhibited significant growth inhibition when subjected to irradiances of 7 W cm^{-2}. In contrast, no growth inhibition was observed for the nanorod-macrophage hybrid spheroids, even at the highest irradiance investigated (28 W cm^{-2}). Growth inhibition was observed at 28 W cm^{-2} when the nanorod concentration was increased, i.e., by forming hybrid spheroids with a 2:1 ratio of glioma cells to macrophages.

Gold nano-spheres are better photo-thermal agents compared to gold nanorods. The work highlights the potential of gold nano-spheres in the treatment of brain tumors using laser-induced photothermal therapy as an adjuvant to conventional therapies.

ACKNOWLEDGEMENTS

I would like to start by thanking my advisor, Dr. Madsen for his guidance and support throughout my work. I would like to also thank my committee members; Dr. Sudowe, Dr. Cerefice and Dr. Alpert for advice and guidance.

I am also grateful for Van Vo and Mary Turner for their technical support, as well as Narek Gharibyan and Balázs Bene for their help in using the UV/Vis spectrophotometry. Finally I would like to thank Dr. Hirschberg at the University of California, Irvine for assistance in treatment setup.

TABLE OF CONTENTS

LIST OF FIGURES

Chapter 1: Introduction

1.1 Glioblastoma Multiforme

Glioblastoma multiforme (GBM) originate from glial cells which are support cells for neurons. GBM is the most common and malignant type of primary brain tumor in adults, and because of its aggressive and invasive nature, there are no effective therapies. With the exception of the brainstem gliomas, GBM has the worst prognosis of any central nervous system (CNS) malignancy (Hart et al. 2008, Martin et al. 2009). Cellular origins and histologic appearance are used as the basis for classifying primary brain tumors. For example, astrocytomas which originate from astrocytes, constitute the majority of CNS tumors (Chandana et al. 2008). Using histologic appearance as the bases for tumor classification, astrocytomas can be graded as pilocytic astrocytoma (grade I), astrocytoma (grade II), anaplastic astrocytoma (grade III), or glioblastoma multiforme (grade IV) (Gomez and Kruse, 2006; Hoelzinger et al. 2007; Hart et al. 2008; Maru et al. 2008; Yamanaka 2008) . Grade I and II tumors are considered low grade while grades III and IV are highly proliferative and have the potential to disperse to distant sites which makes their eradication more difficult than lower grade tumors (Hoelzinger et al. 2007, Chandana et al. 2008). GBM is the most common type of glioma (Figure 1) and the most malignant form of astrocytoma (Gomez and Kruse 2006, Chandana et al. 2008, La Rooca and Mehdorn 2009).

Characteristic features of GBM include large populations of poorly differentiated and pleomorphic cells, endothelial proliferation, tissue invasion, angiogenesis and necrosis. GBM is often resistant to apoptotic stimuli and the tumor cells are not recognized by the immune system. Symptoms are many and varied and are related to

location, size, and growth rate, but they most commonly include seizures, headaches, speech difficulties, and changes in mental status.

GBM is relatively rare (3 cases per 100 000 in the United States) and is more common among Caucasians. In the absence of any form of therapy, median survival is less than three months. With standard therapeutic regimens consisting of surgery, radiation and chemotherapy, median survival ranges from 12 to 18 months (Madsen et al. 2006).

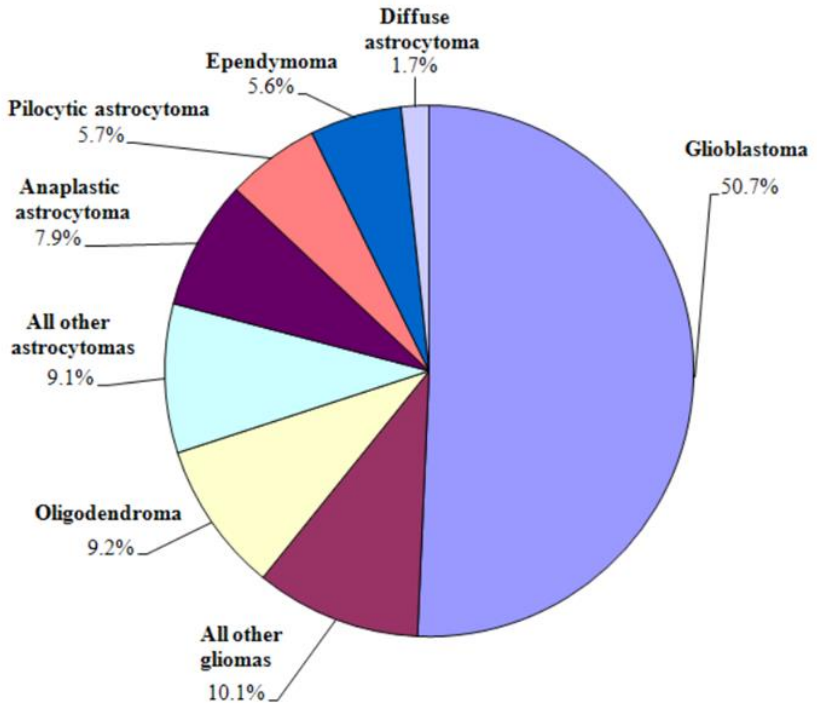

Figure 1: The incidence of CNS gliomas (La Rooca and Mehdorn 2009).

Patients have a high frequency of recurrence due to the highly invasive nature of the tumor: median survival after initial treatment is only 25 weeks, and patients have a relatively poor quality of life due to the detrimental effects of aggressive therapies (Hoelzinger et al 2007). About 90% of GBMs arise from glial cells and are termed primary GBMs. These are more common in older patients and have a typical clinical history of less than 6 months. Secondary GBMs transform over months or years from preexisting lower-grade gliomas and occur predominantly in younger patients (Chandana et al. 2008; Maru et al. 2008; Sathornsumetee and Rich 2008; Reardon and Wen 2006).

1.2 Biology and Molecular Characteristics of GBM

In GBM, there are indications of genetic alterations which include cell cycle regulatory pathways (p53 and p16), growth factor receptors, and signaling pathways (Figure 2). Although primary and secondary GBMs have many genetic abnormalities in common, secondary GBM is characterized by the inactivation of the TP53 gene which is important in inducing cell cycle arrest and initiating DNA repair in response to geno-toxic stress and, as a result, the inactivation is associated with abnormal cell division. Mutations of the tumor-suppressor gene p53 have been reported in 30-60% of malignant gliomas, and are more common in secondary than primary GBMs (Selznick et al. 2008; Yamanaka 2008). Along with TP53 gene inactivation, secondary GBMs have an overexpression of the platelet derived growth factor (PDGF) and its receptors which has been implicated in tumor cell proliferation in both early and late stages of glioma development (Sathornsumetee and rich 2008; Yamanaka 2008; Reardon and Wen 2006). While primary GBM is characterized by overexpression (>60% of cases) of the epidermal growth factor receptor (EGFR) gene, is involved in the control of cell proliferation.

The up-regulation of EGFR has been positively correlated with GBM malignancy, and its defect can also increase activity of an important signaling pathway such as the phosphatidyliositide-3-kinase (PI3K)/AKT pathway which controls cellular processes that contribute to normal homeostasis and malignancy (Figure 2). Primary GBM also exhibits amplification and overexpression of murine double minute 2 (MDM2), a protein which forms a complex with tumor protein 53 (TP53), as a result abolishing the control of cell growth (Selznick et al. 2008).

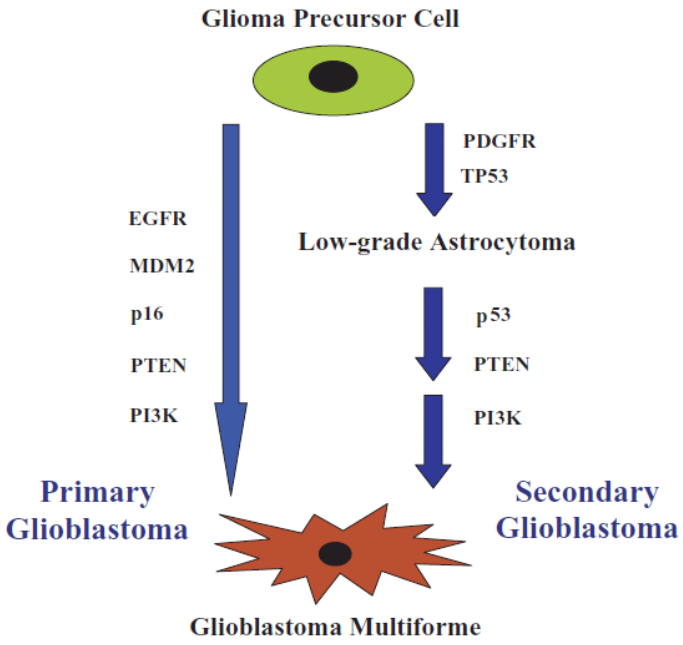

Figure 2: Genetic abnormalities of primary and secondary GBM (Sathornsumetee and Rich 2008)

1.3 Diagnosis and Prognosis

The poor prognosis of GBM patients is due primarily to the infiltrative nature of the disease and despite advances in its management, several factors prevent the complete eradication of GBM. Currently, biopsy is the gold standard for GBM diagnosis since it provides histological information that can be used to determine the potential aggressiveness and hence, mean survival time (Baek et al. 2011; Chandana et al. 2008). With recent advances in imaging, it is now possible to perform deep brain biopsies with accurate tumor localization. Although CT and MRI have been used for diagnosis and treatment planning, these modalities suffer from an inability to accurately delineate tumor margins due to edema build-up associated with the tumor vasculature. The outcome of patients with GBM is influenced by their age, neurological status, tumor location, histological and molecular features and extent of surgical resection. The age of the patient is a significant prognostic factor. Trials have shown that half the patients under the age of 40 survive for 18 months compared to 10% of patients older than 60 (Baek et al. 2011).

The location of the tumor is also an important prognostic indicator: tumors located in the deep gray matter are associated with a better prognosis compared to that of lobar tumors, and patients with frontal lobe tumors have a better prognosis than those with tumors located in the temporal or parietal lobes. A significant limiting factor of GBMs to therapy is their physical isolation by the blood-brain barrier (BBB) which is formed by tightly connected brain capillary endothelial cells. Although this barrier serves a protective function by preventing entry of pathogens into the brain, it also acts as a barrier for anti-cancer agents including chemotherapeutics (Makkouk 2011). Furthermore, tumor resection is greatly hindered by the poor visual contrast between

cancerous and normal brain tissue and an aggressive gross resection often impairs the patient's quality of life while a limited resection may leave residual glioma cells in the margins. Genetic variability is another limiting factor that has created resistance to both chemotherapy and radiation therapy (Gomez and Kruse 2006, Sathornsumetee and Rich 2008; Maier-Hauff et al. 2007; Parvez 2008; Debinski 2008).

1.3.1 Surgery

Following diagnosis, the management of GBM is based on symptomatic relief and increasing survival with multimodality treatments. Currently, the primary treatment for GBM is surgical resection to remove the tumor mass causing the symptoms. The primary goal is to achieve maximal resection while preserving neurological function and, despite being surgically incurable, resection improves functional status and prolongs survival (Parvez 2008). The extent of resection is based on several factors, including location, histopathology, and presence of comorbid conditions. To minimize damage to crucial structures, CT and MRI are used to guide resection in real time to assess tumor volume and delineate critical areas of normal brain (Koo et al. 2006; Reardon and Wen 2006; Chandana et al. 2008; Hart et al. 2008).

1.3.2 Radiation therapy

In almost all cases, resection alone is insufficient and other therapies, including radiation, are employed to destroy malignant cells in the brain adjacent to tumor (Koo et al. 2006; Parvez 2008). For example, randomized studies have shown increases in median survival up to nine months with 50-60 Gy of whole brain radiation following surgery (Reardon and Wen 2006). Radiation therapy can be delivered either externally or

internally. In addition to whole brain irradiation, highly conformal techniques, commonly referred to as stereotactic radiosurgery, are often used for the delivery of high doses to the lesion while sparing normal brain. Interstitial radiation therapy using I-125 seeds implanted into the margin following surgery has also been attempted. This low dose-rate approach may be more effective from a biological point of view compared to the high dose-rate external beam techniques (Chandana et al. 2008; Parvez 2008). Overall, the limitations of radiation include the presence of resistant cells, radiation-induced decline in cognitive function and the risk of secondary malignancies (Koo et al. 2006).

1.3.3 Chemotherapy

The inability of the vast majority of chemotherapeutic agents to penetrate the intact blood-brain barrier has limited their utility in the treatment of brain tumors. (Koo et al. 2006). Furthermore, the problem of multi-drug resistance, resulting in cells actively pumping out therapeutic compounds, has necessitated the use of chemotherapeutic cocktails consisting of a number of compounds (Koo et al. 2006; Hart et al 2008). For example, the standard combination of drugs consisting of Procarbazine, Lomustine, and Vincristine, has been shown in a meta-analysis to be associated with a two month improvement in median survival (Parvez 2008).

Recently, temozolomide (TMZ) has shown significant clinical benefit. GBM patients treated with TMZ and radiation showed median survival of 14.6 months and TMZ has also been shown to be effective as a primary therapy for GBM without a significant risk of early adverse events. The efficacy of this drug is likely associated with its ability to penetrate the intact blood-brain barrier (Hart et al. 2008; Koo et al. 2006).

1.3.4 Laser Interstitial Thermotherapy

The ineffectiveness of current GBM therapies has provided the impetus for the development of new approaches including laser-based techniques such as laser interstitial thermotherapy (LITT) (Menovsky et al.1996). LITT is based on the principle that absorption of light is converted to heat which in turn causes tumor ablation through coagulation. A key to the use of laser irradiation is the ability to localize light delivery (and hence, heat distributions) to the tumor tissue while keeping temperatures in surrounding normal brain below the damage threshold (approximately 43^{o}C). This has traditionally been accomplished via interstitial insertion of optical fibers and thermocouples for feedback control of temperatures in the tumor and normal brain. A more recent, and less invasive approach, makes use of magnetic resonance imaging to monitor real-time temperature distributions during laser heating.

Pre-clinical studies have shown that LITT efficacy depends on a number of factors including laser wavelength. Since tissues (including the brain) absorb strongly at short wavelengths, laser light in the 400-600 nm range is absorbed rapidly resulting in treatment times of the order of several minutes (Kangasniemi et al. 2004). Unfortunately, the rapid increase in energy absorption increases the risk of unintended tissue heating and tissue carbonization which can produce inhomogeneous temperature distributions and unwanted heating of normal tissue (Atsumi et al. 2001). The use of near-infrared absorbing nanoparticles has the potential to improve temperature distributions in tumor tissue and thereby increase the therapeutic efficacy of LITT (Hirsch et al. 2006).

1.4 Nanoparticles

There has recently been an increased interest in the use of nanoparticles in both diagnostic and therapeutic medicine. This is due to a number of factors including the ability to control their shape, size, and synthesis, as well as the ability to manipulate their optical properties (Lin et al. 2005). Gold-based nanoparticles are particularly attractive due to their low toxicity and ease of biomolecule conjugation to their surface (Hirsch et al. 2006; Everts 2007). Nanoparticles such as gold nanorods and nanoshells have been the subject of intense study since their dimensions and/or composition can be tailored for optimum absorption of near-infrared light (Figure 3) which has significant penetration in biological tissues (Huang et al. 2006).

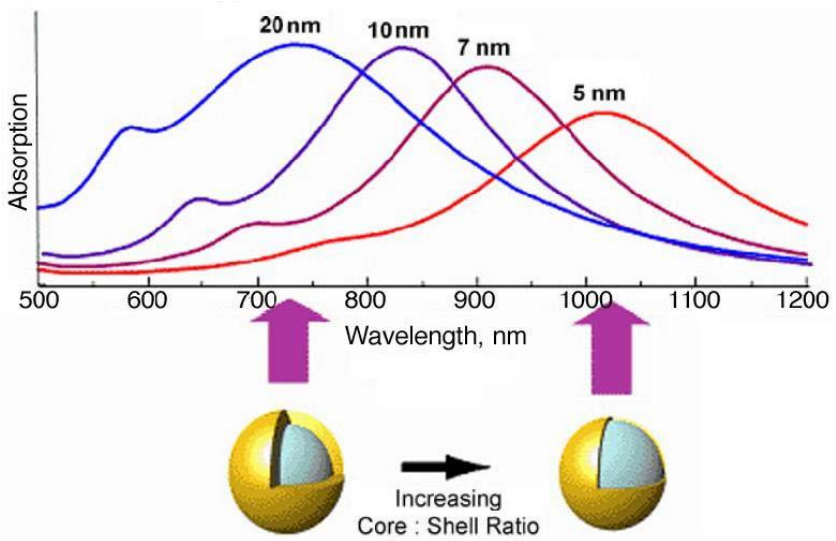

Figure 3: The effect of increasing the core: shell ratio on the plasmon resonance absorption wavelength of gold nano-shells (Hirsch et al. 2006)

Furthermore, compared to photo-thermal dyes, the absorption cross section of nanoparticles can be up to five orders of magnitude higher (Loo 2004). Taken together, these properties can be used to create localized heating or drug release, thus providing the basis for therapeutic applications.

Photon interactions with nanoparticles are dominated by scattering or absorption. For the purposes of therapeutic applications, nanoparticles with high absorption and low scattering cross sections are ideal (Aslan et al. 2005). Light interacts with nanoparticles via the plasmon resonance effect, i.e., the collective oscillation of free electrons at metallic surfaces which causes metallic nanoparticles to absorb and scatter electromagnetic radiation of wavelengths much larger than the particles. Excitation of surface electrons via photon absorption results in a heated electron gas that cools by exchanging its excitation energy with the nanoparticle lattice via electron-phonon interactions. The lattice itself cools within 100 ps by dissipating the energy to the surrounding medium via photon-photon interactions (Huang et al. 2006; Huang et al. 2008).Conversion of light energy to heat is optimized by using a laser at a wavelength that overlaps with the nanoparticle's single plasmonic resonance (SPR) wavelength. This approach has been used in cancer therapeutics and is known as plasmonic photo-thermal therapy (PPTT).

In the case of gold, the plasmon resonance effect is optimal at a wavelength of approximately 520 nm corresponding to green light. A fraction of the incident light is scattered, but the fraction of light absorbed will cause heating thus resulting in a localized increase in temperature, which can be exploited for photo-thermal therapeutic uses (Roco 1999; Cile et al. 2009). Since the peak absorption of gold nanoparticles occurs at a short

wavelength, where tissue penetration is relatively low, their utility in therapeutic applications is rather limited. In contrast, gold nanoshells and gold nanorods have strong absorption in the near-infrared. In the case of nanoshells, the exact absorption peak depends on the ratio of gold shell to silica core thickness: as the shell thickness decreases, the peak absorption shifts to longer wavelengths (Cole et al. 2009). Two absorption bands are observed for gold nanorods; a strong band in the near infrared (NIR) region that is due to the oscillation of electrons along the longitudinal axis, and a weaker band in the visible region due to the transverse electronic oscillation (Huang et al. 2006; Huang et al. 2008). In this case, the peak absorption wavelength depends on the aspect ratio (length-to-width) of the nanorod.

As with any cancer therapy, the goal of nanoparticle-based hyperthermia is the destruction of tumor tissue while avoiding excessive heating of normal tissues - a common problem with well-established hyperthermia techniques such as radiofrequency (RF) and magnetic thermal ablation (Huang et al. 2008; Liu 2008). Tissue heating can be minimized by use of laser radiation of wavelengths in the "tissue optical window" which lies in the visible and NIR regions. Biological tissues lack NIR-absorbing chromophores, which allows optimal transmission of NIR light (700-1000 nm) with minimal heating (Hirsch et al. 2003).

Silica-gold nanoshells have strong and tunable absorption in the NIR region so that the combination of two benign moieties, nanoshells and NIR light, allows for selective heating of tumors loaded with gold nanoparticles. Most PPTT studies have employed diode lasers with wavelengths of 805-810 nm (Terentyuk et al. 2009). In order to achieve thermal ablation, tissues are heated to temperatures in excess of 50^{o} C, where

the tumors are selectively destroyed due to their poor blood supply and subsequent low heat tolerance (Huang et al. 2006).

Optimal PPTT requires preferential localization and/or retention of nanoparticles in tumor tissues. Nanoparticle specificity is a natural consequence of the tumor vasculature which consists of rapidly formed defective vessels with large intercellular gaps ($\leq$ 2 μm) allowing passage of large compounds from the circulation into tumors. This passive process is termed "enhanced permeability and retention (EPR)" (H6irsch et al. 2006; Zaman et al. 2007; Bernardi et al. 2008). Significant accumulation of nanoparticles in tumors via the EPR effect is complicated by their removal from the circulation by macrophages, in particular the Kupffer cells of the liver (Tortora et al. 1995; Cuenca et al.2006; Hirsch et al. 2006; Hamoudeh et al. 2008; Terentyuk et al. 2009). A simple strategy to avoid detection by the immune system is to coat the surfaces of the nanoparticles with a polymer such as polyethylene glycol (PEG) (Hirsch et al. 2006; Everts 2007). Although nanoshell accumulation via the EPR effect has been observed in a wide variety of tumors, it may be insufficient for effective PPTT. This has provided the impetus for the development of "active" approaches including the use of delivery vectors such as macrophages.

1.5 Macrophages

Macrophages are classified as white blood cells that originate from myeloid progenitor cells located in the bone marrow. Monocytes are the precursors that differentiate into macrophages once they migrate from the circulation into the tissue where they reside (Owen et al. 2004; Murdoch and Lewis 2005). Macrophages are the first to mediate host immune responses against foreign objects. Along with their role in

phagocytosis or ingestion of invading pathogens, macrophages also release several growth factors such as cytokines and interleukins (e.g. transforming growth factor-β (TGF-β) and platelet-derived growth factor), and they are involved in a number of other inflammatory responses as well as in the repair of damaged tissues (Metz et al. 2004; Hsiao et al. 2008).

1.5.1 Tumor-Associated Macrophages

In addition to neoplastic cells and blood vessels, tumors are infiltrated by leukocytes, in particular macrophages which represent an important component. These macrophages are known as tumor-associated macrophages (TAMs) which are monocytes that are recruited into the tumor and comprise up to 50% of the tumor's cellular mass (Murdoch and Lewis 2005; Knowles and Harris 2007). In the case of GBM, it has been observed that TAMs can constitute up to a third of the tumor mass. In addition, high concentrations of macrophages are commonly observed along the tumor margins (Jackson et al. 2007; VanHandel et al. 2009). For a tumor to be able to utilize macrophages for their benefit, the macrophages must first be recruited, and to achieve this, tumors induce a chemo attractive gradient by secreting a number of factors, the most important of which are chemokines (Choi et al. 2007).

Many solid tumors are characterized by large hypoxic and/or necrotic regions that occur when the growth rate exceeds the rate of angiogenesis. The necrotic core influences tumor aggressiveness, response to therapy, and the patient's overall survival. The hypoxic cells surrounding the necrotic core adapt by reducing their proliferation rate which renders them less responsive to chemotherapies that kill more active and dividing tumor cells and, as a result, negatively impacts overall survival. Tumor cells in the hypoxic

regions are also less responsive to radiotherapy due to the absence of oxygen-formed free radicals that are important for radiation-induced DNA damage. Interestingly, TAMs have been observed in large numbers in hypoxic tumors where they might be attracted by cells undergoing necrosis.

1.5.2 Use of Macrophages

Macrophages have become a very attractive vector for the delivery of therapeutic agents due to their ability to migrate and accumulate within tumor tissue, specifically in hypoxic regions. Of particular relevance to this work was the recent study by Valable et al. (2009) who injected rats with iron oxide-loaded macrophages followed by magnetic resonance imaging which showed macrophage accumulation in and around brain tumors. An advantage of using such a cell-based delivery system is the increase in the nanoparticles' systemic half-life since the macrophages protect against reticuloendothelial elimination. From a clinical perspective, the basic procedure for such a strategy involves isolation of macrophages from a given patient followed by macrophage loading of the agent of interest (e.g. nanoparticles) which are then injected into the patient (Owen et al. 2004; Murdoch and lewis 2005; Knowles and Harris 2007).

1.6 Spheroids

Three-dimensional spherical cell clusters (spheroids) consisting of a mixture of murine macrophages and human glioma cells were used in this work. Spheroids mimic tumor nodules and metastasis and they have been used to study the effects of therapies on fundamental biological mechanisms including regulation of proliferation, cell death, differentiation, metabolism, invasion, immune response and angiogenesis (Sutherland

1988). In contrast to monolayer cultures, the microenvironment of multicellular spheroids more closely mimics the *in vivo* situation and therefore, gene expression and the biological behavior of the cells are likely similar to that encountered in tumor cells *in situ* (Madsen et al. 2006).

As with solid tumors, spheroids are characterized by significant oxygen gradients resulting in a similar type of cell heterogeneity as observed *in vivo*. For example, a necrotic core forms in spheroids at distances of 50-300 μm from their surface due to inadequate oxygenation. The exact location of the necrotic core depends on a number of factors including cell type, substrate consumption rates, growth media conditions and cell density (Sutherland 1988). In general, the vast majority of proliferating cells are found in the outer three to five cell layers of the spheroid (ca. 75 μm) and a layer of oxygen-starved quiescent cells are found near the necrotic core. These cells can be recruited into the cycling population under the appropriate environmental conditions and, as such, they represent the population of cells resistant to oxygen-dependent therapies such as ionizing radiation and photodynamic therapy (Madsen et al. 2006).

In addition to oxygenation status, tumor response to therapies is controlled by a number of parameters including intracellular contact and communication and susceptibility to apoptosis (Olive and Durnad 1994). Monolayer cultures are inadequate for investigating these parameters as they are unable to mimic oxygen gradients and the complex intracellular adhesion found in 3-D spheroids. Furthermore, the lack of an extracellular matrix in monolayer cell suspensions affects their response to most therapies (Madsen et al. 2006). Since survival and cell death (especially apoptosis) are sensitively dependent on both cell adhesion and the extracellular matrix (Santini et al. 2000), results

obtained in monolayers are likely not a true indicator of *in vivo* therapeutic efficacy, hence providing the rationale for 3-D multi-cell spheroids.

1.7 Scope of Study

The overall objective of the thesis is to compare the PPTT efficacy of gold silica nanoshells and gold nanorods. This was accomplished via two specific aims. In the first part, the uptake efficacy of the two types of nanoparticles was evaluated in murine macrophages. Based on this data, the concentration of nanoparticles will be evaluated in murine macrophages.

The second aim is to investigate the optical to thermal conversion efficacy for the two types of nanoparticles. This was determined by NIR laser irradiation (808 nm) of hybrid spheroids consisting of human glioma cells and nanoparticle-loaded murine macrophages. Overall, PPTT efficacy will be evaluated by monitoring spheroid growth kinetics following laser irradiation. Due to their smaller size, it is hypothesized that nanorod uptake have greater than nanoshell uptake. Additionally, it is hypothesized that the larger nano-shells have a higher optical to thermal conversion efficiency compared to the nano-rods. The overall concept of laser-mediated PPTT using macrophages as vectors for nanoparticles in multicellular spheroids is illustrated in Figure 4.

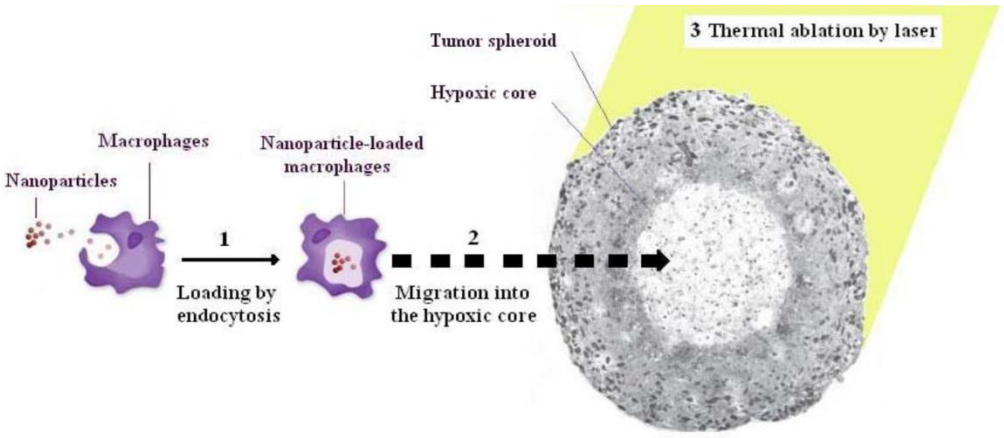

Figure 4: Model of macrophage endocytosis of nanoparticles and incorporation into tumor spheroids followed by laser-mediated thermal ablation (Makkouk and Madsen 2013).

Chapter 2: Materials and Methods

2.1 Cell lines

Two cells lines were used: murine macrophages (P388D1; ATCC# CCL-46) and human grade IV GBM cells (ACBT; G. Granger, University of California, Irvine). Both cell lines were maintained in Dulbecco's Modified Eagle's Medium (DMEM; Life Technologies Corp., Carlsbad, CA) supplemented with 10% fetal bovine serum (FBS), 25 mM HEPES buffer (pH≈7.4), 100 U/mL of penicillin and 100 ug/mL of streptomycin. ACBT is an adherent cell line and is maintained as a monolayer, while the P388D1 macrophage line is grown in suspension. ACBT cells were grown to confluency in an incubator (37^{o} C, 5.0% CO_2 and 95% humidity). The confluent flasks were emptied of media and washed with Gibco phosphate buffered saline (PBS) (Life Technologies Corp., Carlsbad, CA). Cells were detached using Gibco 0.25% Trypsin-EDTA (Life Technologies Corp., Carlsbad, CA) for 5 min. Following detachment a 1:5 dilution of ACBT cells with DMEM, cells were seeded in new T-25 flasks in order to maintain the cell line. In the case of P388D1, the cells were passed at a ratio of 1:100 of P388D1 to DMEM.

2.2 Nanoparticles

Two different types of nanoparticles were used in the study; gold nano-shells (AuroShell™) and gold nano-rods. Both were purchased from Nanospectra Biosciences Inc. (Houston, TX, USA). In both cases, nanoparticles were coated with polyethylene glycol (PEG) in order to prevent aggregation. Gold nanoshells were supplied as a suspension in deionized water (2.82×10^{11} particles/ml), and consisted of a 120-nm

diameter silica core encased in a gold shell of 15 nm thickness giving a total particle diameter of 150 nm. The peak absorption was found at a wavelength of 819 nm (optical density = 105). For the nanorods (length = 45nm; width = 15nm) the stock concentration was 2.0 x 10^{11} particles/mL with a peak absorbance at a wavelength of 765 nm (optical density = 1.09). The absorption spectra for both types of nanoparticles are shown in Figure 5.

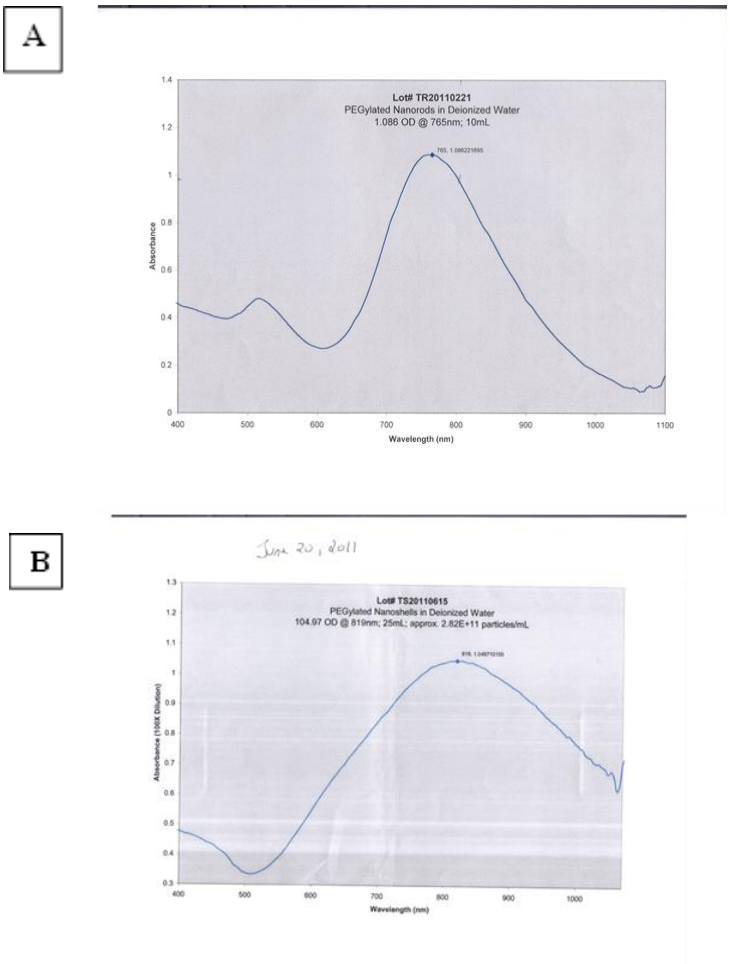

Figure 5: Vis-NIR absorption spectra of (a) pegylated gold nano-shells (top) and (b) pegylated gold nano-rods (bottom).

2.3 Uptake of Nanoparticles

Nanoparticle uptake by macrophages was studied using UV-Vis-NIR spectrometry. Macrophages (5.0×10^6) were incubated with either PEGylated nano-shells (4.3×10^9 per ml) for 24 h or an equivalent concentration of PEGylated nano-rods for varying times ranging from 2 to 36 h. In both cases, incubation was performed under standard conditions (37*C in 5% CO_2 and 95% humidity). Past studies have shown that a concentration of 4.3×10^9 nanoshells/mL and 5 million macrophages was optimal in terms of minimizing toxicity and maximizing uptake (Makkouk 2011). An equivalent nanorod concentration was chosen for comparative purposes.

Following incubation, macrophages were transferred to 15-ml centrifuge tubes, and centrifuged at 600 rpm for 7 min, then washed twice with PBS to remove un-endocytosed particles, while centrifuging and discarding the supernatant in between washes. The final cell pellet was suspended in 3 ml DMEM, and the absorbance of the resultant cellular suspension measured with a Varian UV-Vis-NIR spectrophotometer (Cary 6000i, Varian, USA).

Absorbance was measured over a spectral range of 600-1100 nm, which covers the broad absorption peak of both nanoshells (819 nm) and nanorods (765 nm). To calculate the percentage uptake of nanoparticles, reference solutions containing nanoparticles in absence of macrophages were used, and were prepared in the same solution (media) as that used for macrophage incubation, and at the same dilution ratio. Background correction is necessary to obtain absorbance values corresponding to nanoparticles only i.e. without medium interference. Consequently, solutions prepared by substituting the nanoparticle volume added with DI water were measured, and their

absorbance values subtracted from the nanoparticle solution absorbance values to give the pure absorbance of the nanoparticle.

The absorbance of ingested particles only i.e. without macrophage interference is needed to calculate percentage uptake. Consequently, macrophages incubated under similar conditions (same number, total volume, incubation time) in absence of nanoparticles were similarly washed and suspended in 3 ml DMEM. The resulting solution was measured, and its absorbance values subtracted from those of the macrophage groups to give the pure absorbance of the ingested nanoparticles. The percentage uptake of nanoparticles was calculated by:

$$\frac{A_{M+N}}{A_N} \times 100$$

Where A_{M+N} is the absorbance of endocytosed nano-shells at λ= 819 nm (or nanorods at 765 nm), and A_N is the absorbance of the reference nanoshell (or nanorod) solution at the same wavelength.

2.4 Hybrid Spheroid Formation

Hybrid spheroids were formed using human ACBT cells and P388D1 murine macrophages. Nanoparticles (4.3×10^9 per ml) were incubated with macrophages (5.0×10^6 per ml) under standard conditions 24 h prior to the formation of hybrid spheroids. After 24 h of incubation, macrophages were washed twice with PBS in order to remove non ingested nanoparticles. Prior to the formation of hybrids, macrophages were treated with mitomycin C to prevent macrophage division. Hybrid spheroids consisting of ACBT cells and empty macrophages served as controls.

On the day of spheroid formation, ACBT cells (70% confluence) were harvested from the growth flasks and transferred to a centrifuge flask. A solution of 5000 ACBT cells/ml (10 ml total) and solutions of loaded (or unloaded) macrophages (both at 1000 cells/ml were prepared. A 5:1 ACBT:macrophage solution was created by adding 5 ml ACBT cells to 5 ml of loaded macrophages. Finally, 200 µl of the mixture was pipetted into a 96-well plate for a final solution of 5000 ACBT cells and 1 000 macrophages per well. In one study, the effects of increasing the nanorod-loaded macrophage concentration were investigated. This was accomplished by decreasing the number of ACBT cells and increasing the macrophage number while keeping the total number of cells constant. In this case, 4000 ACBT cells were mixed with 2000 loaded macrophages. In all cases, the well plates were centrifuged at 1000 rpm for 10 min and thereafter hybrid spheroids were incubated under standard conditions for 48 hours. Following incubation, spheroid diameters typically ranged between 400 and 450 µm. At this point, the spheroids were prepared for laser irradiation.

2.5 PPTT Treatment

Prior to laser irradiation, spheroids were transferred to a clean 96-well plate (one spheroid per well). Every second well was left empty in order to minimize light scatter to non-irradiated spheroids. Prior to spheroid transfer, each well was filled with 200 µl DMEM. Irradiation was performed using a high power 808 nm diode laser (HPD-7404; Intense, North Brunswick, NJ). The output of the diode laser was coupled into a 600-µm dia. core optical fiber containing a collimating lens at its output end (FD1; Medlight, Ecublens, Switzerland). An additional lens assembly was attached to the fiber in order to focus the beam to the 3 mm diameter required for the experiments. Due to limitations of

the laser output (approx. 2 W), the high irradiances (up to 28 W cm^{-2}) required for the experiments could only be achieved by focusing the beam. This posed a significant time constraint since only one spheroid could be irradiated at any given time. The output end of the optical fiber was placed in contact with the bottom of the well and each spheroid was irradiated for 10 min. at irradiances of 2, 7, 14 or 28 W cm^{-2}, The laser power was monitored every 20-30 min. and adjusted accordingly. Treatment efficacy was monitored from spheroid growth kinetics. This was accomplished by measuring spheroid diameters using an ordinary light microscope with a calibrated eyepiece. Measurements were made every 2-3 days over a 15day period. The DMEM medium was changed twice weekly during the observation period.

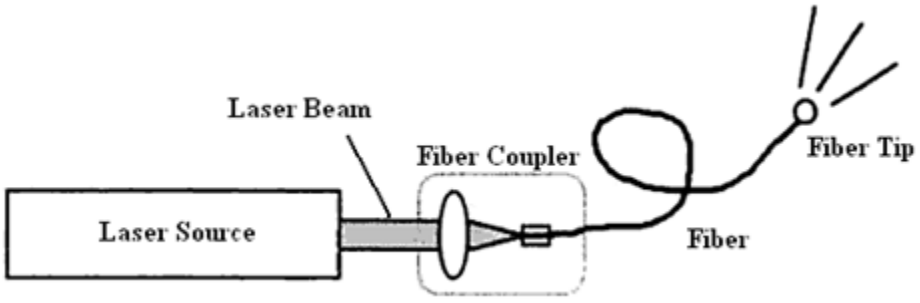

Figure 6: Components of the laser system (Van Gemert MJC, 1995).

Chapter 3: Results

3.1 Uptake of nanoparticles by murine macrophages

As illustrated in Figure 7, the uptake of nanorods by murine macrophages is greater than nanoshell uptake. Following 24 hours incubation, spectrophotometric analysis revealed uptakes of 3.9 ± 0.9 and 7.9 ± 0.7% for nanoshells and nanorods, respectively. Based on the initial nanoparticle concentrations, these uptakes correspond to 337 nanoshells and 680 nanorods per macrophage, respectively. A p value of 0.04 was determined from a t-test between the mean nanoparticle values per macrophage. This suggests, the difference in uptake was statistically significant at the 95% confidence interval.

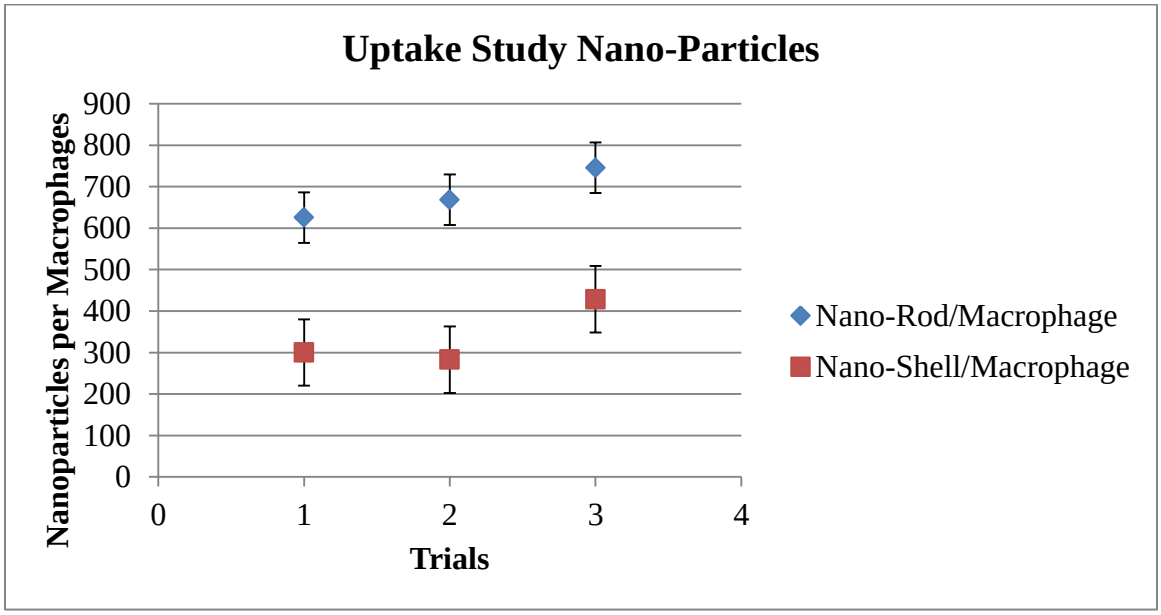

Figure 7: Comparison of gold nanoshell and gold nanorod uptake by murine macrophages. Equal concentrations of gold nanoshells and nanorods were incubated with macrophages for 24 h and uptake was evaluated from spectrophotometric analysis. The uptake difference was statistically significant ($p < 0.05$).

A study was initiated to determine whether nanorod uptake could be improved by increasing incubation times. The results are illustrated in Figure 8 and they show a rapid increase in uptake over the first 6 hrs, followed by a gradual increase to the 18 h time point. A rapid drop in uptake was observed for incubation times exceeding 24 h. Overall, the results provide justification for the 24 h incubation time as this is near optimal.

3.2 Photothermal therapy of nanoparticle-loaded hybrid spheroids

In order to rule out the possibility of laser-induced thermal effects, control spheroids consisting of ACBT cells and empty macrophages were irradiated. The results (Figure 9) show minimal growth inhibition at all irradiances compared to the non-irradiated controls. Spheroids in all five control groups grew to a diameter of approximately 1 mm at the end of the 14-day observation period. Overall, the results show that laser-induced thermal effects were insignificant over the range of irradiances investigated.

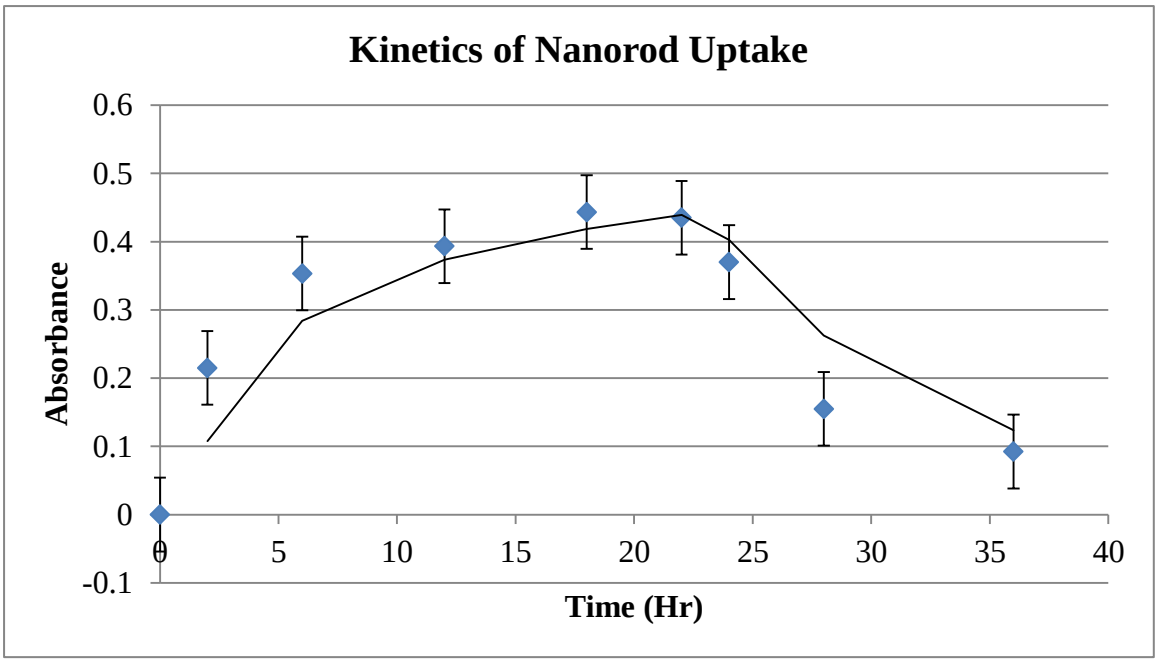

Figure 8: Uptake kinetics of nanorods by murine macrophages. Absorbance at 765 nm was used as a marker for nanorod uptake. Each data point corresponds t**o** the mean of three trials and error bars denote standard deviations.

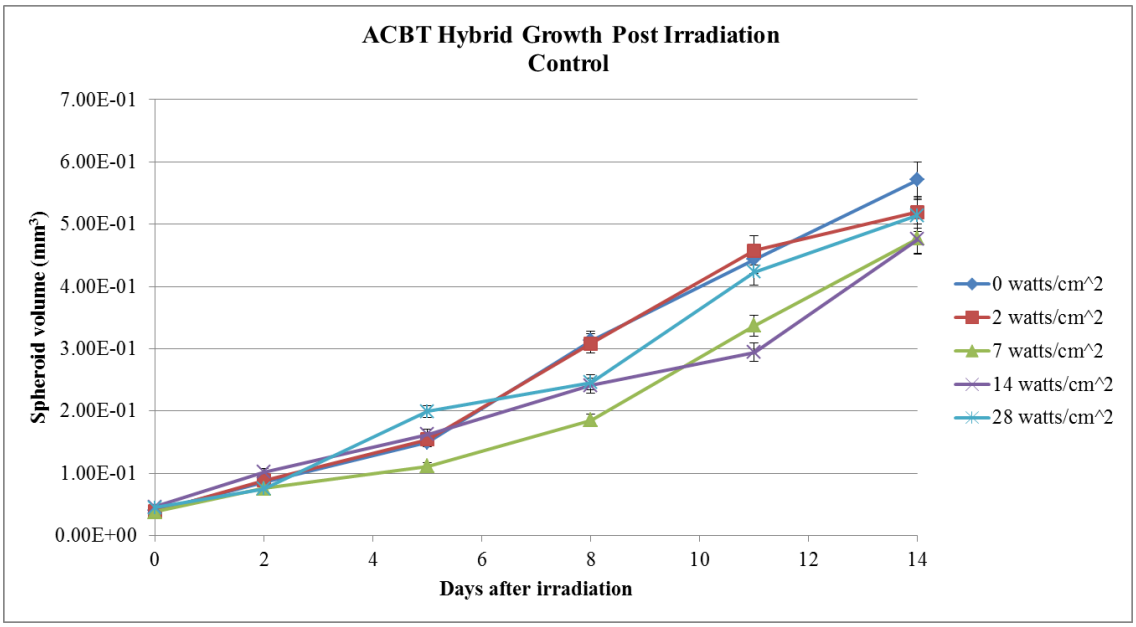

Figure 9: Growth kinetics of hybrid spheroids consisting of 5000 ACBT cells and 1000 empty murine macrophages were monitored. Following exposure to varying irradiances. Each data point represents the mean of three experiments and the error bars denote standard deviations. Growth kinetics was monitored over 2 weeks.

Survival of nanoshell- and nanorod-loaded hybrid spheroids exposed to a range of laser irradiances are illustrated in Figure 10. No cytotoxicity was observed at the lowest irradiance investigated (2 W cm^{-2}). In the case of the nanoshell-loaded spheroids, significant decreases in spheroid survival were observed at irradiances of 7 W cm^{-2} and higher. Spheroid survival was approximately 63, 56 and 40% at irradiances of 7, 14 and 28 W cm^{-2}, respectively. In the case of the nanorod-loaded spheroids, no significant diminution in survival (compared to empty hybrid controls) was noted at any of the irradiances investigated including the highest irradiance corresponding to 28 W cm^{-2}.

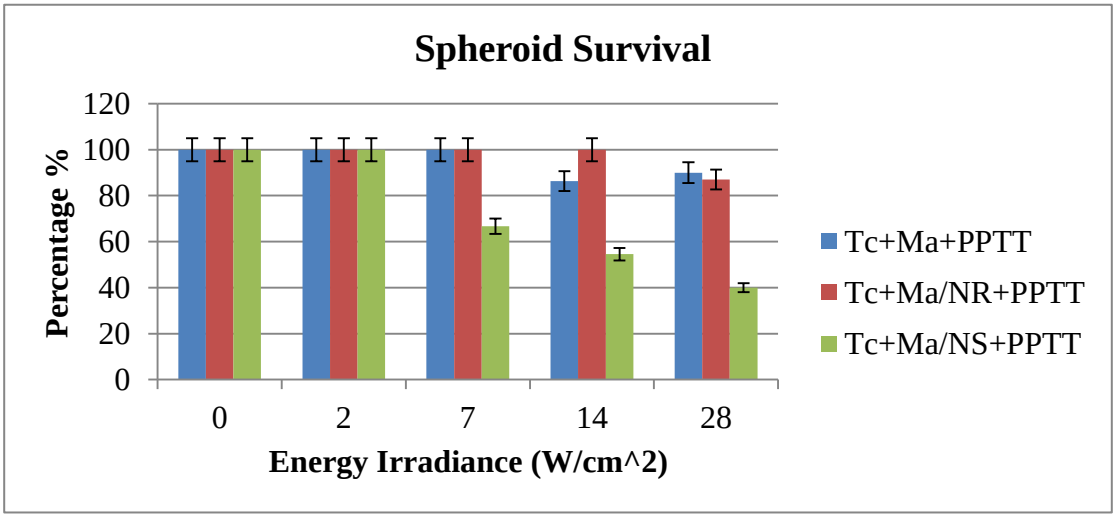

Figure 10: Survival of hybrid nanoshell (Tc+Ma/NS+PPTT) and nanorod (Tc+Ma/NR+PPTT) spheroids as a function of 808 nm laser irradiance. Tc+Ma+PPTT denote hybrid control spheroids consisting of empty macrophages. Each data point corresponds to the mean of three trials and error bars denote standard deviations.

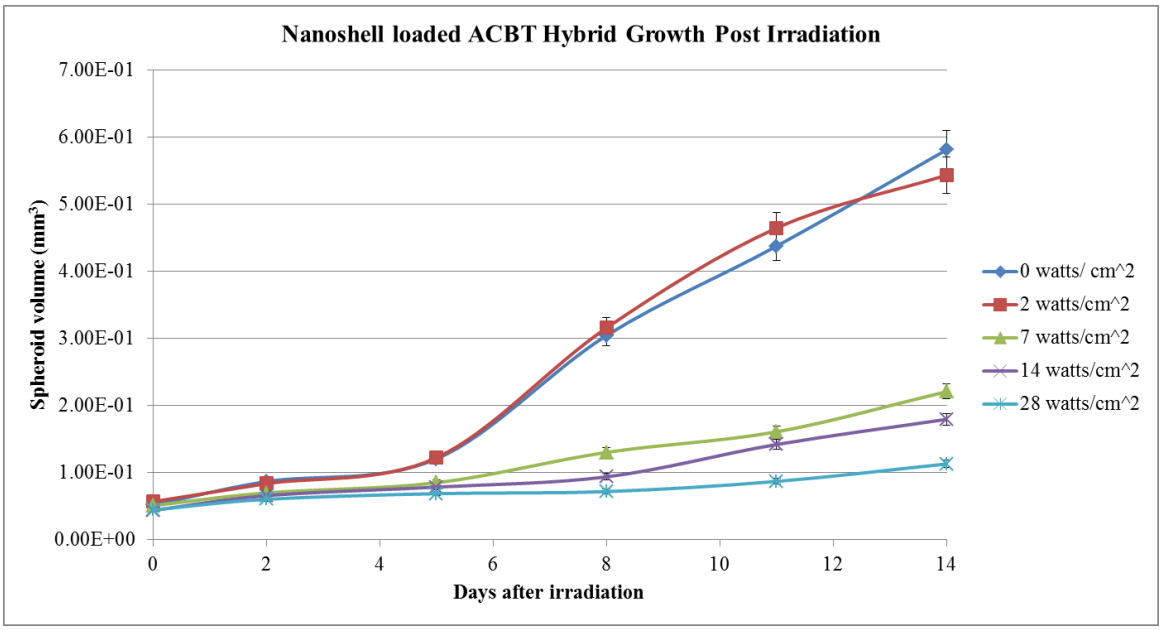

Figure 11: Growth kinetics of nanoshell-loaded spheroids. Each data point corresponds to the mean of three experiments and error bars denote standard deviations.

The growth kinetics of surviving nanoshell-loaded hybrid spheroids are shown in Figure 11. Compared to non-irradiated controls, significant growth delays were observed in hybrid spheroids subjected to irradiances ≥ 7 W cm^{-2}.

The growth kinetics of nanorod-loaded hybrid spheroids subjected to a range of near infrared laser irradiances are illustrated in Figure 12. The data show that, over the range of laser irradiances investigated, no statistically significant growth delays were observed compared to non-irradiated controls. Spheroids in all treatment and control groups reached a diameter of approximately 1 mm at the end of the 2 week observation period.

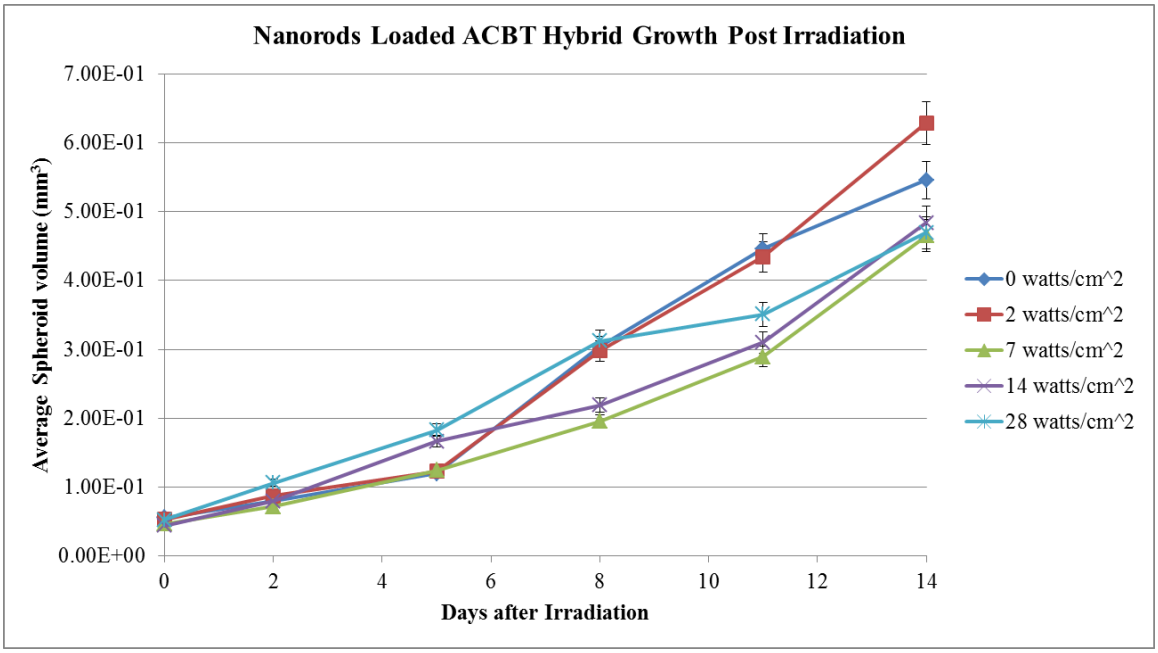

Figure 12: Growth kinetics of nanorod-loaded spheroids. Each data point corresponds to the mean of three experiments and error bars denote standard deviations.

An attempt was made to determine whether a thermal effect could be induced by increasing the number of nanorod-loaded macrophages in each spheroid. To that end, hybrid spheroids consisting of 4000 ACBT cells and 2000 nanorod-loaded macrophages were exposed to an irradiance of 28 W cm^{-2}. The data presented in Figure 13 show a doubling of the number of nanorod-loaded macrophages results in a significant decrease in survival. For example, laser irradiation of hybrid spheroids consisting of 1000 nanorod-loaded macrophages resulted in 87% survival which was not statistically different from the survival of the empty hybrid control spheroids (90%). In contrast, laser exposure of hybrid spheroids consisting of 2000 nanorod-loaded macrophages resulted in 62% survival. Although a significant thermal effect was observed by doubling the number of nanorod-loaded macrophages, it was not as pronounced as the effect observed

for the spheroids containing 1000 nanoshell-loaded macrophages where exposure to 28 W cm^{-2} resulted in a survival of 40%.

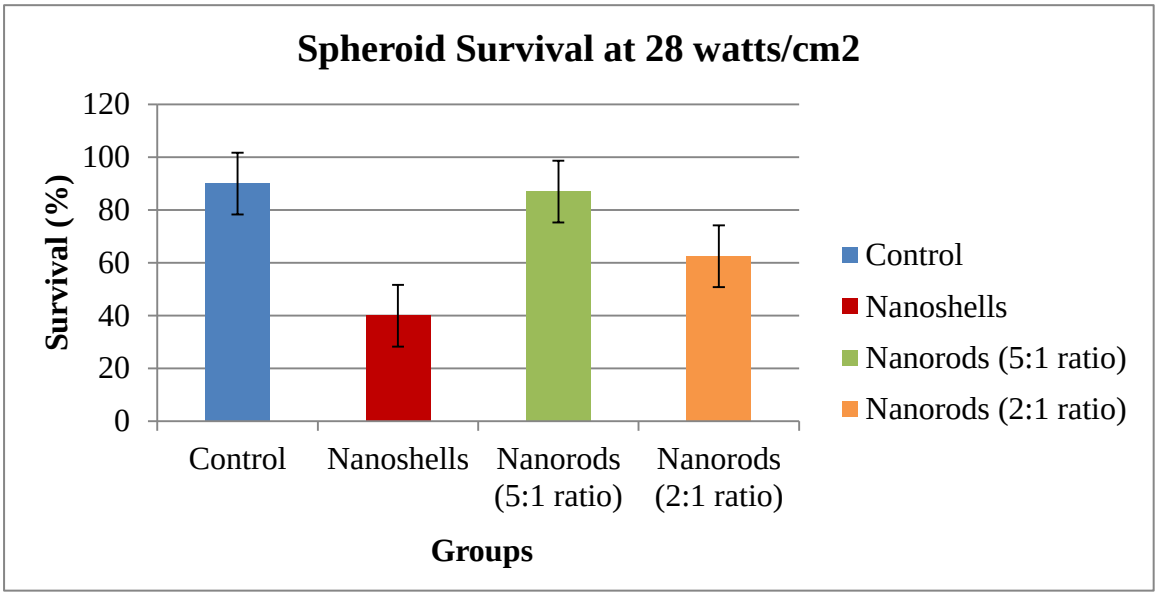

Figure 13: Hybrid spheroid survival as a function of nanorod-loaded macrophage concentration. All spheroids were subjected to 808 nm laser irradiation at an irradiance of 28 W cm^{-2} and survival was recorded on day 14 post-irradiation. Each data point corresponds to the mean of three trials and error bars denote standard deviations.

Chapter 4: Discussion

A number of *in vitro* and *in vivo* studies have been performed to evaluate the potential of gold-based nanoparticles for PPTT of brain tumors. Most studies have focused on gold-silica nanoshells as their properties are well characterized in comparison to other formulations (Makkouk and Madsen 2013). The first reported use of nanoshells for PPTT of brain tumors occurred in 2008 when Bernardi et al. (2008) used two different antibody conjugated nanoshells to target overexpressed receptors in high-grade human glioma and human medulloblastoma cell lines. Selective destruction of tumor cells overexpressing the selected biomarkers was observed following near infrared laser exposures of 9.6 kJ cm^{-2}.

A different targeting approach was investigated by Baek et al. (2011) who used macrophages as delivery vectors for gold-silica nanoshells. The *in vitro* model used by this group (hybrid spheroids consisting of human ACBT glioma cells and murine macrophages) was identical to that used in this work and the laser irradiation parameters provided the rationale for those used in the present study. Significant effects on spheroid growth were observed at near infrared laser irradiances as low as 7 W cm^{-2} (radiant exposure of 4.2 kJ/cm^2). Overall, these findings are in excellent agreement with the results obtained in the present study showing significant spheroid growth inhibition at irradiances $\geq$ 7 W cm^{-2} (Figure 11).

Cabada et al (2012) investigated the efficacy of gold nanorod-mediated PPTT in a high-grade human glioma cell line. They observed significant cell death following near infrared laser exposures of 1.4 kJ. Cell death was attributed to plasma membrane damage. A direct comparison with the results obtained in the present work is not possible due to

differences in the *in vitro* models (monolayer vs. spheroid) and the lack of information concerning intracellular nanorod concentrations in the monolayer model. Based on the results presented in Figure 13, much higher laser exposures were required to produce noticeable spheroid death (16.8 kJ/cm^2 vs. 1.4 kJ/ cm^2 for the monolayers).

Of the two reported *in vivo* gold nano-shell PPTT brain tumor studies, one used a murine model (Day et al. 2011) while the other was accomplished in canines (Schwartz et al. 2009). In the latter study, tumors were established by injecting canine transmissible venereal tumor cells into canine brains. Passive accumulation of gold silica nano-shells was observed in tumors 24 h post i.v. administration. Thereafter, intracranial near infrared laser irradiation (0.63 kJ) resulted in near complete tumor ablation, with minimal damage to adjacent normal tissue. This study, in particular, provides the rationale for clinical trials.

Although two in vivo gold nanorod PPTT studies have been reported (Dickerson et al. 2008; Von Maltzahn et al. 2009) neither involved brain tumor models. Nevertheless, both studies demonstrated significant tumor regression in murine models following near infrared laser irradiation of gold nanorod-loaded tumors.

The delivery of nanoparticles to brain tumors is complicated by the presence of the BBB which protects the brain from circulating pathogens. Unfortunately, it also prevents entry into the brain of the vast majority of anti-cancer agents including the large nanoparticles investigated in this work. Although these nanoparticles are capable of entering brain tumors via passive diffusion through the leaky tumor vasculature (the EPR effect), the resultant intra-tumor distribution is often quite heterogeneous therefore providing the rationale for alternative delivery approaches such as those using exogenous

macrophages (Valable et al. 2007). Although such a technique might prove useful for destroying the tumor mass, its ability to eliminate nests of infiltrating glioma cells that have migrated into normal brain remains uncertain since these cells are protected by the patent BBB. A recent study by Madsen et al. (2013) demonstrated that exogenously administered nanoparticle-loaded macrophages were unable to traverse the BBB in normal rat brains suggesting elimination of infiltrating glioma cells requires targeted opening of the BBB prior to macrophage administration. This could be accomplished using a variety of targeted approaches including ultrasound, photodynamic therapy or photochemical internalization (Madsen and Hirschberg, In Review).

Macrophages are efficient scavengers of pathogens and therefore it was hardly surprising that both types of gold nanoparticles were phagocytized by murine macrophages. As illustrated in Figure 7, approximately twice as many nanorods were ingested compared to nanoshells. The explanation for this observation is uncertain since the biophysical mechanisms of phagocytosis have not been well studied. The few studies that have been published have focused primarily on polymer micro-particles since these are similar in size to biologic pathogens (Champion et al. 2008). It is well established that size, shape and surface chemistry influence phagocytosis (Beningo and Wang 2002; Champion and Mitragotri 2006; Ahsan et al. 2002).

For example, smaller particles are more readily phagocytized than larger ones as are particles with shapes similar to pathogens such as bacteria. Both of these observations would explain the results presented in Figure 7. The effects of surface chemistry on phagocytosis have been studied extensively. It is well known that the addition of a polyethylene glycol coating impairs phagocytosis by delaying opsonization, or adsorption

of proteins which enhance phagocytosis (Owens and Peppas 2006). It is precisely for this reason that PEGylated nanoparticles are used for *in vivo* applications – reduced macrophage uptake increases bio-distribution times and nanoparticle concentrations in target tissues. Both types of gold nanoparticles used in the studies described herein were PEGylated to prevent aggregation. Additional stabilization of nanorods was accomplished by the addition of small amounts of Cetyl trimethylammonium bromide (CTAB) thus altering the surface chemistry in comparison to the nanoshells.

The addition of CTAB might explain the data in Figure 8 which show a significant decrease in absorbance for incubation times exceeding 24 hours. High concentrations ($\geq$ 3.6 μg ml^{-1}) of CTAB coated gold nanorods have been shown to be cytotoxic to human glioma cells (Fernandez Cabada et al. 2012). Although the concentration of CTAB nanorods used in the present studies (0.34 μg ml^{-1}) was approximately 10 times lower, it's possible that this was close to the cytotoxic limit since nanoparticle uptake by macrophages is expected to be much more efficient compared to uptake by glioma cells. It's likely that, for incubation times exceeding 24 hours, the number of internalized CTAB nanorods exceeded the cytotoxicity threshold for murine macrophages. The effects of CTAB on macrophage viability could be investigated by removing the coating with hydrochloric acid (HCl).

Silica core gold nanoshells and gold nanorods are the two most commonly used nanoparticles in PPTT (Young et al. 2012). The resonant coupling of incident light to the collective oscillation mode of the conduction electrons of noble metal nanoparticles (termed surface Plasmon resonance effect) produces enhancement in the optical absorption. It may also cause scattering when the particle is larger than a few tens of

nanometers. The optical response of metallic nanoparticles can be calculated from Maxwell's equations, however, due to their computational complexity, approximations are typically used including Mie theory for spheres and the discrete dipole approximation for non-spherical geometries such as rods (Young et al. 2012). These models can be used to design scatter dominated or highly absorbing particles for diagnostic or therapeutic applications, respectively.

Based on theoretical calculations, nano-spheres are predominantly scattering particles while extinction by nano-rods is primarily due to absorption. For example, calculations show that the nanoshells and nanorods used in the present work absorb approximately 12 and 93% of the incident light, respectively (Cole et al. 2009). However, nano-shells have a much larger cross-sectional area (and therefore a larger photothermal transduction cross-section) compared to the nanorods. Based on calculations by Jain et al. (2006), the absorption efficiency of the nanoshells used in this work is approximately ten times greater than that of the nanorods. Since the absorption efficiency is equivalent to the photothermal transduction efficiency (ignoring aggregation effects), this implies, the ratio of gold nanorods to nanoshells required for equivalent photothermal effect is 10:1.

The PPTT results presented in Figures 10-13 are in good qualitative agreement with theoretical predictions. For example, the data show that, on a per nanoparticle basis, gold nanoshells have a higher photothermal transduction efficiency as determined from spheroid survival and growth inhibition. The nano-shell data presented in Fig. 10 is in good agreement with Baek et al (2011) who also found diminished spheroid survival at irradiances $\geq$ 7 W cm^{-2}. In contrast, photothermal effects were minimal, or non-existent, for the nanorod-loaded spheroids over the irradiances investigated (Figures 10 and 12).

This is hardly surprising based on the nanorod-to-nanoshell ratio (2:1) in the hybrid spheroids as determined from the uptake studies shown in Figure 7.

The effects of increased nanorod concentration were investigated by doubling the number of nanorod-loaded macrophages from 1000 (5:1 ACBT: macrophages) to 2000 (2:1 ACBT: macrophages). As shown in Figure 13, increasing the nanorod-to-nanoshell ratio to 4:1 from 2:1, resulted in a decrease in spheroid survival by approximately 20%. As expected, even at this higher nanorod concentration, PPTT was less efficient compared to nanoshell PPTT as determined from spheroid survival (40% vs. 61%). As discussed previously, based on theoretical calculations, a nanorod-to-nanoshell ratio of approximately 10:1 is required for equivalent photothermal effects. Attempts to increase nanorod uptake by increasing incubation times were unsuccessful (Figure 8). Increasing the number of macrophages (and hence nanorods) was not attempted since this would likely result in unstable spheroid formation – macrophages are not known to form spheroids and therefore there is a practical limit to the number that can be used in hybrid spheroid formation.

The results obtained in this work reinforce the findings of other studies showing that PPTT is not a very efficient treatment modality. As illustrated in Figure 10, a noticeable diminution in survival is only observed at radiant exposures $\geq$ 4.2 kJ cm^{-2} corresponding to an irradiance of 7 W cm^{-2} and an irradiation time of 10 min. In comparison, significant photodynamic therapy effects in identical ACBT spheroids are observed at radiant exposures of only 2.5 J cm^{-2}. In this context, it is difficult to envision the use of PPTT for the treatment of large tumor masses such as GBM where surgical resection is likely to remain the primary treatment. PPTT may be useful as an adjuvant

therapy for eliminating malignant cells in the resection margin and beyond following surgical resection. PPTT may also be useful for smaller, well-circumscribed lesions (e.g. brain metastases) since it can be delivered locally via interstitially implanted optical fibers thereby minimizing damage to surrounding normal brain. This is likely to result in a better quality of life compared to that achievable with standard therapies such as ionizing radiation.

Chapter 5: Conclusion

The purpose of this work was to compare the efficacy of gold nanoshells and nanorods in PPTT using a GBM spheroid model. Nano-rods are much smaller compared to nano-shells and this is likely the reason for their increased uptake by murine macrophages, e.g., the results presented herein show that nanorod uptake was approximately twice that of nano-shells for equivalent incubation times and particle concentrations. It was not possible to increase nanorod loading by using longer incubation times and, in fact, the standard 24 hours incubation period was near optimal. The sharp decline in nanorod uptake for incubation times exceeding 24 hours was attributed to CTAB-induced macrophage toxicity. Although relatively high laser irradiances were used in this work (7 – 28 W cm^{-2}), they did not produce noticeable thermal effects in hybrid spheroids devoid of nanoparticles. A significant decrease in nanoshell-loaded spheroid survival was noted at irradiances of 7 W cm^{-2}. In this case, the total energy delivered (radiant exposure) over the 10 min. irradiation period was 4.2 kJ cm^{-2}. Spheroid viability decreased with increasing irradiance, ranging from 63% at 7 W cm^{-2} to 40% at 28 W cm^{-2}. Significant growth inhibition was also observed for surviving nanoshell spheroids at irradiances $\geq$ 7 W cm^{-2}, with the greatest inhibition noted for the highest irradiance.

Laser exposure of nanorod-loaded spheroids did not produce statistically significant differences in either survival or growth kinetics compared to controls. A decrease in spheroid survival was only observed following a doubling of the number of nanorod-loaded macrophages. In this case, the total number of nano-rods exceeded that of nano-shells by a factor of four. Even at this higher nanorod concentration, PPTT was less

efficient (61% viability) compared to that obtained for the lower concentration nanoshell spheroids (40%).

Overall, the results show that, on a per nanoparticle bases, gold-silica nano-spheres have a greater photothermal efficiency compared to gold nano-rods. Theoretical calculations suggest the ratio of nano-rods to nano-shells required for equivalent PPTT effect is somewhat higher (approximately 10:1) than the 4:1 ratio used herein and this was likely the reason PPTT equivalency was not observed in these studies.

A potential avenue for future research involves strategies for increasing nanorod uptake by murine macrophages. This could be accomplished simply by chemical removal of CTAB. If this approach fails to yield increased nanorod uptake, an alternative strategy to increase the nanorod-to-nanoshell ratio might be accomplished by deliberately decreasing nanoshell uptake, e.g., by decreasing incubation times. In either case, the goal would be to increase the nanorod-to-nanoshell ratio to 10:1, i.e., the ratio where theoretical calculations predict an equivalent effect for the two types of nanoparticles.

Reference

Aslan K, Lacowicz J, Geddes CR. Plasmon light scattering in biology and medicine: new sensing approaches, visions and perspectives. Curr.opin.Chem.Biol 9(5): 1367-5931; 2005

Ahsan FL, Rivas IP, Khan MA, and Suarez AI. "Targeting to macrophages: Role of physicochemical properties of particulate carriers—liposomes and microspheres—on the phagocytosis by macrophages." J Control Release 79: 29-40; 2002

Atsumi H, Matsumae M, Kaneda M, Muro I, Mamata Y. Novel laser system and laser irradiation method reduces the risk of carbonization during laser interstitial thermotherapy: assessed by MR temperature measurement. Lasers Surg Med 29(2): 108-112; 2001

Baek S, Amani Riad Makkouk, Tatiana Krasieva, Madsen SJ. Photothermal treatment of glioma; an in vitro study of macrophage-mediated delivery of gold nanoshells. J Neurooncol 104(2): 439-448; 2011

Beningo KA, Wang YL. Fc-receptor-mediated phagocytosis is regulated by mechanical properties of the target. J Cell Sci 115: 849-856; 2002

Bernardi RJ, Lowery AR, Thompson PA, Blaney SM. Immunonanoshells for targeted photothermal ablation in medullablastoma and glioma: an in vitro evaluation using human cell lines. J Neurooncol 86(2): 165-172; 2008

Cabada F, De Pablo CS, Serrano AM, del Pozo Guerrero F, Javier Serrano Olmedo J, Gomez MR. "Indcution of cell death in a glioblastoma line by hyperthermic therapy based on gold nanorods." int. J. nanomedicine: 1511-1523; 2012

Champion JA, Amanda Walker, Samir Mitragotri. "Role of Paricle Size in Phagocytosis of Polymeric Microspheres." Pharmaceuticla Research 25(8): 1815-1821; 2008

Champion JA, Mitragotri S. "Role of target geometry in phagocytosis." Proc Natl Acad Sci U S A 103: 4930-4934; 2006

Chandana SR, Movva S, Arora M, Sing T. "Primary brain tumors in adults." American Family Physician 77(10): 1423-1430; 2008

Cheung KL, Chen H, Chen Q, Wang J, Ho HP, Wong CK, Kong SK. "CTAB-coated gold nanorods elicit allergic response through degranulation and cell death in human basophils." Nanoscale 4(15) : 4447-4449; 2012

Choi JH, Nguyen FT, Barone PW, Heller DA, Moll AE, Patel D. "Multimodal biomedical imaging with asymmetric single-walled carbon nanotube/iron oxide nanoparticle complexes." Nano Lett 77(10): 861-867; 2007

Cile J, Mirin N, Knight M.. "Photothermal efficiencies of nanoshells and nanorods for clinical therapeutic application." J Phys Chem 113(28):12090-12094; 2009

Cole JR, Mirin NA, Knight MW, Goodrich GP, Halas NJ. "Photothermal efficiencies of nanoshells and nanorods for clinical therapeutics applicaitons." J Phys Chem 113: 12090-12094; 2009

Cuenca AG, Jiang H, Hochwald SN, Delano M, Cance WG, Grobmyer SR. "Emerging implications of nanotechnology on cancer diagnostics and therapeutics." Cancer 107(3):459-466; 2006

Daniel MC, Astruc D. "Gold Nanoparticles: assembly, supramolecular chemistry, quantum-size-related propertis, and applicaiton toward biology, catalysis, and nanotechnology." Chem. Rev 104: 293-346; 2004

Day ES, Thompson PA, Shang L, Lewinski N.A., Ahmed N., Drezek R.A., et al. "Nanoshell-mediated photothermal therapy improves survival in a murine glioma model." Journal of Neuro-Oncology 104(1): 55-63; 2011

Debinski W. "Drug cocktails for effective treatment of GBM." Expert Rev. Neurother 8(4): 515-517; 2008

Dickerson EB, Dreaden EC, Huang X, El-Sayed IH, Chu H. "Gold nanorod assisted near-infrared plasmonic photothermal therapy (PPTT) of squamous cell carcinoma in mice." Cancer Lett 296(1): 57-66; 2008

Everts M. "Thermal Scalpel to target cancer." Expert Rev.Med.Devices 4(2): 131-136; 2007

Folkman J, Hochberg M. "Self-regulation of growth in three dimensions." J.Exp.Med 113(4): 745-753; 1973

Gobin AM, Moon JJ, West JL. "EphrinAI-targeted nanoshells for photothermal ablation of prostate concer cells." Int J Nanomedicine 3(3): 351-358; 2008

Gomez GG, Kruse CA. "Mechanisms of malignant glioma immune resistance and sources of immunosuppression." Gene Ther.Mol.Biol 10 (A): 133-146; 2006

Hamoudeh M, Kamleh MA, Diab R, Fessi H. "Radionuclides delivery systems for nuclear imaging and radiotherapy of cancer." Adv.Drug Deliv.Rev 60(12): 1329-1346; 2008

Hart MG, Grant R, Garside R, Rogers G, Somerville M, Stein K. "Temozolomide for high grade glioma." Cochrane Database Syst.Rev. 4(4): CD007415; 2008

Hirsch LR, Gobin AM, Lowery AR, Tam F, Jalas NJ. "Metal nanoshells." Ann.Biomed.Eng 334(1): 15-22; 2006

Hirsch LR, Stafford RJ, Bankson JA, Sershen SR, Rivera B, Price RE. "Nanoshell-mediated near-infrared thermal therapy of tumors under magnetic resonance guidance." Proc.Natl.Acad.Sci.U.S.A. 100 (23): 13549-13554; 2003

Hoelzinger Db, Demuth T, Berens ME. "Autocrine factors that sustain glioma invasion and paracrine biology in the brain microenvironment." J.Natl.Cancer Inst. 99(21): 1583-1593; 2007

Hsiao JK, Chu HH, Wang YH, Lai CW. "Macrophage physiological function after superparamagnetic iron oxide labeling." NMR Biomed 21(8): 820-829; 2008

Huang X, El-Sayed IH, Qian W, El-Sayed MA. "Cancer cell imaging and photothermal therapy in the near-infrared region by using gold nanorods." J.Am.Chem.Soc 128(6): 2115-2120; 2006

Huang X, Jain PK, El-Sayed IH, El-Sayed MA. "Plasmonic photothermal therapy (PPTT) using gold nanoparticles." Lasers Med.Sci 23(3): 217-228; 2008

Jackson H, Muhammad O, Daneshvar H, Nelms J, Popescu A, Vogelbaum MA. "Quantum dots are phagocytized by macrophages and colocalize with experimental gliomas." Neurosurgery 7(4): 524-529; 2007

Jain PK, Lee KS, El-Sayed I. "Calculated Absorption and Scattering Properties of Gold Nanoparticles of Different Size." J.Phys.Chem 110: 7238-7248; 2006

Julie A. Champion, Amanda Walker, Samir Mitragotri. "Role of Paricle Size in Phagocytosis of Polymeric Microspheres." Pharmaceuticla Research 25(8): 1815-1821; 2008

Kah JC, Wan RC, Wong KY, Mhaisalkar S, Sheppard CJ, Olivo M. "Combinatorial treatment of photothermal therapy using gold nanoshells with conventional photodynamic therapy to improve treatment efficacy: an in vitro study." Lasers Surg Med 40(8): 584–589; 2008

Kah JC, Wong KY, Neoh KG. "Criticla parametres in the pegylation of gold nanoshellos for biomedicla applications: an in vivtro macrophage study." Journal of Drug Target 17(3): 181-193; 2009

Kangasniemi M, McNichols RJ, Bankson JA, Gowda A, Price RE. "Thermal therapy of canine cerebral tumors using a 980 nm diode laser with MR temperature-sensitive imaging feedback." Laser Sug: 35-41;(2004)

Knowles HJ, Harris AL. "Macrophages and the hypoxic tumor microenvironment." Fromt.Biosci: 4298-4314; 2007

Koo YE, Reddy GR, Bhojani M, Schneider R, Philbert MA, Rehemtulla A. "Brain cancer diagnosis and therapy with nanoplatforms." Adv.Drug deliv.Rev. 58(14): 1556-1577; 2006

La Rooca RV, Mehdorn HM. "Localized BCNU chemotherapy and the multimodal nanagement of malignant glioma." Curr.Med.Res.Opin. (1): 149-160; 2009

Lin AW, Lewinski NA, West JL, Halas NJ, Drezek RA. "Optically tunable nanoparticle contrast agents for early cancer deterction: Midel-based analysis of gold nanoshells." J.Biomed.Opt 10(6): 064035; 2005

Liu C, Mi CC, Li BQ. "Energy absorption of gold nanoshells in hyperthermia therapy." IEEE Trans.Nanobioscience 7(3): 206-214; 2008

Loo C, Lin A, Hirsch L, Lee MH, Halas N, West J, Drezek R. "Nanoshells-enabled photonics-based and therapy of cancer." Technol. Cancer Res: 33-44; 2004

Love JC, Estroff L, kriebel J. "Self-assembled monolayers of thiolates on metals as a form of nanotechnology." Chem. Rev.: 1103-1169; 2005

Madsen SJ, Sun CH, Tromberg BJ. "Multicell Tumor Spheroids in Photodynamic Therapy." Lasers in Surgery and Medicine 38: 555–564; 2006

Madsen SJ, Gach HM, Uzal FA, Hirschberg H. "Increased nanoparticle-loaded exogenous macrophage migration into the brain following PDT-indcued blood-brain barrier disruption." J. Neurooncol : In review

Madsen SJ, Hirschberg H. "Site-specific opening of the blood-brain barrier." J. Biophotonics 3(5-6): 356-367; 2010

Maier-Hauff K, Rothe R, Scholz R, Gneveckow U. "interacranial thermotherapy using magnetic nanoparticles combined with external beam radiotherapy: results of a feasibility stydy on patient with GBM." J.Neurooncol 81(1): 53-60; 2007

Makkouk, AR. "Macrophage loaded with gold nanoshells for photo thermal ablation of glioma: an in vitro model." ProQuest, UMI Dissertation Publishing (September 30, 2011) University of Nevada, Las Vegas, NV.

Makkouk, AR, and Madsen SJ. "Nanoparticle-mediated Photothermal Therapy of Brain Tumors." Optical Methods and Instrumentation in Brain Imaging and Therapy. Vol. 3. New York: Springer, 2013. 235-51

Marites P. Melancon, Wei Lu, Zhi Yang, Rui Zhang, Zhi Cheng. "In vitro and in vivo targeting of hollow gold nanoshells directed at epidermal growth factor receptors for photothermal ablation therapy." Mol Cancer Ther 7(6): 1730-1739; 2009

Martin V, Liu D, Gomez-Manzano C. "Encountering and adcancing through antiangiogenesis therapy for gliomas." Curr.Pharm.Des. 15(4): 353-364; 2009

Maru SV, Hollyway KA, Flynn G, Lancashire CL, Loughlin AJ, Male DK. "Chemokine prodcution and chemokine receptor expression by human glioma cells: role of CXCL10 in tumor cell proliferation." J.Neuroimmunol. 199(1-2): 35-45; 2008

Menovsky T, Beek JF, Roux FX, Bown SG. "Interstitial laser thermotherapy: developments in the treatment of small deep-seated brain tumors." Surg. Neurol 46(6): 568-571; 1996

Metz S, Bonaterra G, Rudelius M, Settles M, Rummeny EJ, Daldrup-Link HE. "Capacity of human monocytes to phagocytose approved iron oxide MR contrast agents in vitro." Eur.Radiol 14(10): 1851-1858; 2004

Murdoch C, Lewis CE. "Macrophage migration and gene expression in response to tumor hypoxia." Int.J.Cancer 117(5): 701-708; 2005

Olive PL, Ralph E. Durand. "Drug and radiation resistance in spheroids: cell contact and kinetics." Cancer and Metastasis Reviews 13(2): 121-138; 1994

Owen MR, Byrne HM, Lewis CE. "Mathematical Modeling of the use of macrophages as vehicles for drug delivery to hypoxic tumor sites." J.Theor.Biol 226(4): 377-391; 2004

Owens DE, III, Peppas NA. "Opsonization, biodistribution, and pharmacokinetics of polymeric nanoparticles." Int J Pharm 307: 93-102; 2006

Parvez, T. "Present trend in the primary treatment of aggressive malignant glioma: glioblastoma multiforme." Technol.Cancer.Res.Treat. 7(3): 241-248; 2008

Perez-Juste J, pastoriza-Santos I, Liz-Marzan L. "gold nanorods synthesis, characterization and applications." Coord. Chem Rev 7 (3): 1870-1901; 2006

Pissuwan D, Valenzuela S, Cortie M. "Therapeutic Possibilities of plasmonically heated gold nanoparticles." TRENDS in Biotechnology 24(2): 62-67; 2006

Reardon DA, Wen PY. "Therapeutic advances in the treatment of glioblastoma: rationale and potential role of targeted agents." Oncologist 11(2): 152-164; 2006

Roco MCE. "Nanoparticles and Nanotechnology Research." Journal of Nanoparticle Research 1(1): 1-6; 1999

Sathornsumetee S, Rich JN. "Designer therapies for glioblastoma multiforme." Ann.N.Y.Acad.Sci. 1142: 108-132; 2008

Santini MT, Rainaldi G. "Apoptosis, cell adhesion and the extracellular matrix in the three-dimensional growth of multicellular tumor spheroids." Critical Reviews in Oncology/Hematology 36(2-3); 75-87; 2000

Schwartz JA, Shetty AM, Price RE, Stafford RJ, Wang JC, Uthamanthil RK. "Feasibility study of particle-assisted laser ablation of brain tumors in orthotopic canine model." Cancer Res. 15, (69): 1659-1667; 2009

Selznick LA, Shamji MF, Fecci P, Gromeier M, Friedman AH, Sampson J. "Molecular strategies for the treatment of malignant glioma-genes, viruses, and vaccines." Neurosurg.Rev 31(2): 141-155; 2008

Sershen SR, Westcott JC, Halas NJ. "Temperature-sensitive polymer-nanoshell composites for photothermally modulated drug delivery." J. Niomed. Matter: 293-298; 2000

Sutherland R. "Cell and Environment Interactions in Tumor Microrgegions: The Multicell Spheroid Model." American Association for thet Advancement of Science 240: 177-184; 1988

Sutherland R, Carlsson J, Durand R. "Spheroids in Cancer Research." Cancer Research 41: 2980-2984; 1981

Sutherland, RM. "Cell and environment interactions in tumor microregions: the multicell spheroid model." Science 240: 177-184; 1998

Tamara Fernandez Cabada, Cristina Sanchez Lopez de Pablo, Alberto Martinez Serrano. "Induction of cell death in a glioblastoma line by hyperthermic therapy based on gold nanorods." Int J Nanomedicine 7: 1511-1523; 2012

Terentyuk GS, Maslyakova GN, Suleymanova LV, Khlebtsov NG, Khlebtsov BN, Akchurin GG. "Laser-induced tissue hyperthermia mediated by gold nanoparticles: toward cancer phototherapy." J.Biomed.Opt 14(2): 021016; 2009

Tortora GJ, Funke BR, Case CL. "Microbiology. an introdcution. 5th edition. Redwood City, CA: Benjamin/Cummings Publishing, CO., INC., 1995

Valable S, Barbier E, Bernaudin M, Roussel S, Segebarth C. "In vivo MRI tracking of exogenous monocytes/macrophages targeting brain tumors ini a rat model of glioma." NeuroImage 37: S47-S58; 2009

Van Gemert MJC, Welch AJ, Pickering JW. Optical Thermal Response to Laser Irradiated Tissue. New York: Plenum Press, 1995.

VanHandel M, Alizadeh D, Zhang L, Kateb B, Bronikowski M, Manohara H. "Selective ptake of multi-walled carbon nanotubes by tumor macrophages in a murine glioma model." J.Neuroimmunol 208(1-2): 3-9; 2009

Varun P. Pattani, James W. Tunnell. "Nanoparticle-Mediated Photothermal Therapy: A comparative Study of Heating for Different Particle Types." Lasers in Surgery and Medicine 44: 675-684; 2012

Von Maltzahn G., Park J.H., Agrawal A., Bandaru N.K., Das S.K., Sailor M.J., Bhatia. "Computationally guided photothermal tumor therapy using long-circulating gold nanorod antennas." Cancer Res 69: 3892-3900; 2009

Wang B, Yantsen E, Larson T. "Plasmonic intavascular photoacoustic imaging for detection of macrophages in atherosclerotic plaques." Nano Letters 9(6): 228-235; 2008

Yamanaka, R. "Cell and peptide based immunotherapeutic approaches for glioma." Trends Mol.Med 14(5): 228-235; 2008

Young JK, Figueroa ER, Drezek RA. "Tunable nanostructures as photothermal theranostic agents." Ann biomed Eng 40: 438-459; 2012

Zaman RT, Diagaradjane P, Wang JC, Schwartz J, Rajaram N, Gill-Sharp KL. In Vivo Detection of Gold nanoshells in Tumors Using Diffuse Optical Spectroscopy. Selected Topics in Quantum Electronics. IEEE Journal 13(6): 1715-1720; 2007

VITA

University of Nevada, Las Vegas
School of Allied Health Sciences, Health Physics Department

Suyog J. Chhetri

Degrees:

Bachelor of Science, 2009
Purdue University, West Lafayette IN

Thesis Title:

Efficacy of Gold silica nano-shells and gold nano-rods for photothermal therapy of human glioma spheroids

Thesis Examination Committee:

Committee Chair, Dr. Steen Madsen, Ph.D.
Committee Member, Dr. Ralf Sudowe, Ph.D.
Committee Member, Dr. Gary Cerefice. Ph.D
Graduate Faculty Representative, Dr. Patricia T. Alpert, DrPH